International Journal of Recent Engineering Research and Development (IJRERD)
Volume No. 02 – Issue No. 01, ISSN: 2455-8761
www.ijrerd.com, PP. 31-41

Investigation of nanostructure of a new Fast ionic Conductor [Cu_2CdI_4:0.xRbI] where (x = 0.1, 0.2 and 0.3 mol. wt. %)

Noorussaba[†] and A. Ahmad[†]*

[†]Solid State Chemistry Lab, Department of Chemistry,
Aligarh Muslim University, Aligarh- 202002, India.

Abstract: Considerable effort has been taken to the development of new Rb^+ ion conducting composite fast ionic systems, [Cu_2CdI_4:0.xRbI] (where x = 0.1, 0.2 and 0.3 mol. wt. %), were prepared, using [Cu_2CdI_4] mixed composite system as the host. [Cu_2CdI_4] compound belongs to the fast ion conductors of A_2BX_4 (A = Ag, Cu, B = Hg, Cd, Zn, Pb and others). The compound [Cu_2CdI_4] becomes superionic near 388K as the crystal lattice changes from a tetragonal to a hexagonal structure. Near 445K, [Cu_2CdI_4] is replaced by an equilibrium mixture of α- CuI and CdI_2. At each of these phase transition, ionic conductivity increases by an order of magnitude or more. The substitution of Cd^{++} from Rb^+ in [Cu_2CdI_4] is accompanied by a slight increase in the room temperature conductivity, as a result of either increased crystalline defects or an increased Rb^+ substitution also characterized. FTIR, FAR-IR, SEM and EDAX analyses were performed to confirm the formation of fast ion conductors [Cu_2CdI_4:0.xRbI] (where x = 0.1, 0.2 and 0.3 mol. wt. %).

Keywords*:* **A**. FTIR; **B**. FAR-IR; **C**. SEM; **D**. EDAX; **E**. Doping; **F**. Fast ion conductors.

1. Introduction

Many fast ionic compounds including those belonging to the A_2BX_4 group (A = Ag and Cu, B = Cd and Hg, X = I) are usually obtained by means of ceramic technology [1-4]. Chemical substitution has been used extensively in recent years to modify either the magnitude of ionic conductivity or the transition temperature separating super ionic and covalent phases in various solid electrolytes [5]. Present work is based on the study of some nominal compositions of [Cu_2CdI_4:xRbI] where x = 0.1, 0.2, 0.3 mol. wt. % respectively using the differential thermal analysis (FTIR), and analyses differential scanning calorimetry (FAR-IR), thermal gravimetric analysis (SEM), Fourier transmission infrared spectra (EDAX) and x-ray powder diffraction (XRD) techniques. Cu_2CdI_4 is a solid electrolyte having hexagonal structure. Cu_2CdI_4 has a conductivity value 10-6 (ΩCm)-1 at room temperature but there are two phase transitions β – γ phase above 276oC [6]. R. Sudharsanan et. al studied the Raman and Far IR measurements on the Cu_2CdI_4 compounds at room temperature to elucidate the conduction mechanism in this matetials [5]. Recently Khalid Siraj, has reported ionic conductivity in Ag and Na substituted Cu_2CdI_4 [7]. The temperature dependent thermochromism is due to changes in the charge transfer spectra arising from the donation of electron charge from the filled p-orbitals of the iodide ligands to the unfilled d-orbitals of the cadmium atom. The phase transition is considered to be an order-disorder type. The low temperature, β-phase for Cu_2CdI_4 are tetragonal but they differ in the placement of the Cu+ cations and vacancy. In the high temperature, α- phase, the iodide sublattice is retained while cations are distributed randomly among all sites. Thus, (A_2BX_4) are isostructural in their α-phases, clearly, them, the Cu^+ cations plays a role in the exact structure in the low temperature form and determines, for the most part, the conductivity, phase transition temperature and thermo chromic properties [8]. We have undertaken a study of the synthesis and properties of the analogues of Cu_2CdI_4 with the overall objective to finetune the structural, spectral and thermal properties of Cu_2CdI_4 compounds with the choice of possible mixed (Rb^+) substitutions to obtain materials useful for sensors and others electrochemical devices. Although the initial purpose of this work is to see cations double (Rb^+) effect by introducing in Cu_2CdI_4 systems, we find that it is quit difficult to see this and instead we find the structure of pure Cu_2CdI_4 systems is different from iodide fast ionic system leading to the phase separation structure [9].

This paper is a part of our investigation on the synthesis, and characterization of Rb^+ cation substituted [Cu_2CdI_4]. In, the present investigation, Although the initial purpose of this work is to see cations (i.e. Rb^+) effect by introducing in A_2BX_4 systems, we find that it is quit difficult to see this and instead we find the structure of pure A_2BX_4 systems is different from iodide fast ionic system leading to the phase separation structure.

SERIES OF SAMPLES:

e.g. 1) [Cu_2CdI_4:xRbI] -

a) [Cu_2CdI_4]
b) [Cu_2CdI_4:1RbI]
c) **[**Cu_2CdI_4:2RbI]
d) **[**Cu_2CdI_4:3RbI]

In the [A_2BX_4] where (A = Cu, B = Cd and X = I) systems [A_2BX_4] are pure materials, In [A_2BX_4:xRbI] composite system (where x = 0.1, 0.2, 0.3 mol. wt. %, A = Cu, B = Cd, and X = I), [A_2BX_4] considered as host doped with [xRbI] (where x = 0.1, 0.2, 0.3 mol. wt. %) as the dopant. The composition of the host [A_2BX_4] was kept constant in all the composite samples of [A_2BX_4:xRbI]. It has been observed that a much better solid electrolyte composite system can be prepared with the host [A_2BX_4] (A = Cu, B = Cd and X = I) systems] [10].

Experimental Procedure

2.1. Material

The following materials were used as received; copper (I) iodide and cadmium [II] iodide were of CDH anal grade, each of which had a purity of 99.5%, 99.2% respectively.

2.2. Preparation and characterization of pure and doped samples

2.2.1. Preparation of pure [Cu_2CdI_4] host sample

Copper tetraiodocadmiate [Cu_2CdI_4] was prepared by the conventional solid state reaction from CuI and CdI_2 (CDH, India), with stated purity of 99.5 and 99.2% respectively. Both reactants i.e. CuI and CdI_2 were mixed in a requisite composition (according to eqn no.2)

$$2CuI + CdI_2 \rightarrow Cu_2CdI_4 \qquad (2)$$

in an Agate mortar and were heated at 300°C (573K) for 48 hrs in a silica crucible with intermittent grinding. The heating rate was initially kept at 50°C per hrs for 12 hrs. The product so formed was cooled slowly at room temperature

2.2.2. Preparation of doped sample [Cu_2CdI_4:0.xRbI]

RbI were mixing in various x = 0.1, 0.2 and 0.3 mol. wt. % respectively in an Agate motar to form [Cu_2CdI_4:xRbI] composite mixture by solid state reaction. Silver tetra-iodocadmiate 02 mol. wt. % [Cu_2CdI_4] were doped by 0.1, 0.2 and 0.3 mol. wt. % (RbI) dopant solid respectively to form [Cu_2CdI_4:0.xRbI] fast ion conductor, in an Agate mortar at room temperature and heating them at 100°C (373K) for 24 hrs in a silica crucible. After intermittent grinding, all the samples were prepared [11].

2.3. Characterization of [Cu_2CdI_4:0.xRbI] composite fast ion conductor

The novel composite fast ion conductors [Cu_2CdI_4:0.xRbI], were prepared and investigated by Scanning electron microscopic (SEM), energy disperssive spectral (EDAX), FTIR spectral analysis to confirmed the formation of all the fast ion conductors.

2.3.1. Scanning electron microscopic (SEM) Studies

The scanning electron microscopic (SEM) studies were performed to get information about homogeneity, particle distribution and morphology of all the fast ionic composite systems [Cu_2CdI_4:xRbI] (where x = 0.1, 0.2 and 0.3 mol. wt. %) after the reaction was completed using Jeol JSM 6510LV Scanning Electron Microscope at room temperature and different magnifications (at 3000x and 10,000x).

2.3.2. Energy dispersive spectral (EDAX) Studies

Chemical analysis of a [Cu_2CdI_4:0.xRbI] (were 0.1, 0.2 and 0.3 mol. wt. %) processed samples was carried out by EDAX to check if there is any deviation from the initial composition. Fig. 4 shows a typical EDAX result for [Cu_2CdI_4:0.xRbI] sample.

2.3.3. Far-IR Spectral Analysis

The Far-IR spectrum was recorder for all the fast ionic composite systems [Cu_2CdI_4:xRbI] (where x = 0.1, 0.2 and 0.3 mol. wt. % respectively) in the far-infrared range 30-400 cm^{-1} at room temperature using a Perkin Elmer/ FTIR Spectrometer measured in KBr. The far-infrared spectral region is the range of wavenumbers

where one finds many of the large-amplitude anharmonic vibrations. These include both the symmetric and asymmetric internal torsional modes of many small organic and organometallic molecules.

2.3.4. FTIR Spectral Analysis

The IR spectrum was recorder for all the fast ionic composite systems [Cu_2CdI_4:xRbI] (where x = 0.1, 0.2 and 0.3 mol. wt. %) in the mid-infrared range 400-4000 cm^{-1} (25-25 μm) at room temperature using a INTERSPEC-2020, FTIR spectrophotometer measured in KBr. Mid–infrared spectra used to study the fundamental vibrations and associated rotational-vibrational structures.

3. Results and discussion

3.1. FTIR analysis

3.1.1. FAR-IR discussion in [Cu_2CdI_4:0.xRbI]

. The IR spectrum of the vapour over solid [Cu_2CdI_4:0.xRbI] (where x = 0.1, 0.2 and 0.3 mol. wt. %) was studied in the 30-700 cm^{-1} region at room temperature are shown in figure 1.

The IR spectrum of [Cu_2CdI_4:0.xRbI] where x = 0.1, 0.2 and 0.3 mol. wt. %) solid at room temperature showed two distinct absorption bands. The absorption around 102.10, 113.64, 109.10 cm^{-1} in x = 0.1, 0.2 and 0.3 mol. wt. % shows typical PR band structure of a diatomic molecule and is assigned to the fundamental Ag-I stretching frequency of the monomer. For the band origin at 83.36, 71.89 and 91.54 cm^{-1} in x = 0.1, 0.2 and 0.3 mol. wt. % can be attributed to the $(CuI)_2$ dimeric molecule respectively [12]. IR- measurements shows that a sifnificant amount of dimeric molecules is present in the vapour over AgI at the temperature of the present experiments.

Ionic model calculations based on Rittners electrostatic model [13] predicted a square planar structure (D_{2h} symmetry) as the most stable arrangement for $(CuI)_2$. This structure allows three of the total six normal modes of vibration to be IR active. The B_{2u} and B_{3v} stretching modes involve high frequency in plane motion and the B_{1u} bending mode lower frequency out of plane motion. On the basis of these consideration the peak at 83.36, 71.89 and 91.54 cm^{-1} in x = 0.1, 0.2 and 0.3 mol. wt. % is due to the stretching motion and the peak at ca 57.31, 58.52 and 72.06 in x = 0.1, 0.2 and 0.3 mol. wt. % is due to the bending motion of the $(CuI)_2$ molecule. There is however, no clear argument for the assignment of the observed stretching band to the B_{2u} and B_{3v} mode [13].

The spectrum of [Cu_2CdI_4:0.xRbI] where x = 0.1, 0.2 and 0.3 mol. wt. %) solid consisted of two strong absorption bands are listed in Table 1. It is concluded that both peaks are due to CdI_2 molecular species. The linear structure of the CdI_2 molecule ($D_{\infty h}$ symmetry), as established by electron diffraction measurements [14-16], allow two of the total of three fundamental frequencies to be infrared active and consequently, the assignment is straight forward, the symmetric Cd-I stretching frequency υ_3 at 228.81, 229.21, 229.99 cm^{-1} in x = 0.1, 0.2 and 0.3 mol. wt. % and I-Cd-I blending frequency υ_2 at 136.56, 152.67, 151.76 cm^{-1} in x = 0.1, 0.2 and 0.3 mol. wt. %. The additional sharp lines in the spectrum are due to the rotational spectrum of H_2O impurities. The IR spectrum of [Ag_2CdI_4:0.xRbI] where x = 0.1, 0.2 and 0.3 mol. wt. %) solid composite, also shows three distinct absorption bands at 318.20, 466.72 and 621.35 $cm^{-1,}$ in x = 0.1, 317.39, 455.72 and 628.45 $cm^{-1,}$ in x = 0.2, 319.02, 469.14 and 614.86 $cm^{-1,}$ in x = 0.3. On further increasing the wavenumber the position of the absorption bands are in excellent agreement with those of the [Cu_2CdI_4] molecules [17] above 400 cm^{-1}, the intensity of the peaks decreases, owing to condensation of CdI_2 in the colder parts of the optical cell, these bands corresponds to those AgI and indicate the presence of AgI and $(CdI_2)_2$ molecules.

In addition, numerous sharp absorption bands of the rotational spectrum of [Cu_2CdI_4:0.xRbI] where x = 0.1, 0.2 and 0.3 mol. wt. %) were presents, which were at 656.37, 686.20 $cm^{-1,}$ in x = 0.1, 537.73, 611.39, 653.02, 671.69 cm^{-1} in x = 0.2, 545.11 and 664.75 cm^{-1} in x = 0.3 mol. wt. %. These absorption bands are in excellent agreement with those of the [Cu_2CdI_4] host composite. Additional peaks that might indicate the presence of Rbl species is at 203.31, 251.23, 269.10 cm^{-1} in x = 0.1, 189.47, 269.05 cm^{-1} in x = 0.2, 191.13, 270.13 cm^{-1} in x = 0.3 mol. wt. % have been observed shows Rb-I stretch of the molecule.

The present results shows that the successive release of CdI_2 and $CuI/(CdI_2)_2$ vapour species occurs during heating, pointing towards dissociation of [Cu_2CdI_4:0.xRbI] where x = 0.1, 0.2 and 0.3 mol. wt. %) molecules under the conditions of the experiments (Table 1). Additional peaks that might indicate the presence of Cu-Cd-I species have been observed.

3.1.1. FTIR discussion in Cu_2CdI_4

As in Ketelaar description, the α- phase retains the same iodine structure as in the β phase. While the cation and vacancy sites becomes equivalent [18]. Later studies [19, 20] showed that the low temperature phases are tetragonal and in addition, are not isostructural, differing in the placement of the two monovalent cation (Ag or Cu) and vacancy. Thus based on data from the best single crystals, i.e. tetragonal β- phase was the only stable

low-temperature phase and the apparent phase change after cycling could be explained by the formation of domains with the tetragonal c axis randomly oriented along the three spatial axes, thus giving the impression of a cubic lattice. The interpretation of a single low-temperature phase has the broadest base of support of the two views at present [20]. Assuming the β phase is tetragonal, the number and symmetry of normal modes can be determined. Group theory analysis finds the following number and symmetries for the 18 optical modes in Cu_2CdI_4 materials.

Cu_2CdI_4: 3A+ 5B+ 5E

The Infrared and Raman selection rules give the following allowed mode symmetries.

Infrared	Raman
Cu_2CdI_4: 5B+ 5E (10 Bands)	3A+ 5B+ 5E (13 Bands)

Using projection operators, we find that the B symmetry mode involve motion of the cation along the tetragonal c axis (z), and the E modes involve motion of the cations, along the a and b axes (x or y), B mode couple to electric fields along the z axis and E modes couple to fields in the xy plane, so that FTIR spectra would determine the mode-symmetry assignments uniquely [21-23].

3.1.2. Factor group analysis of Cu_2CdI_4

The irreducible representation for the 10 IR allowed modes are listed in Table 2. The unit cell group analysis of Cu_2CdI_4 is also shown in Table 2 [25], with the D_{2d} - S_4 correlation being A_1 and A_2 to A, B and B_2 to B and E to E. Figure 2 shows FTIR spectrum for [Cu_2CdI_4:0.xRbI] fast ionic conductors where x = 0.1, 0.2 and 0.3 mol. wt. %.

In the IR spectra of [Cu_2CdI_4:0.xRbI] the 2931.09 cm^{-1} peak in Table 2 is strongest in xx, yy and zz direction making it an A. The A peak shifted in x = 0.2 and 0.3 mol. wt. % at 2931.09, 2927.05 cm^{-1}. The peak at 1349.91 cm^{-1} are strongest in the xx and yy polarizations and therefore belongs to B classes. This peak shifted in x = 0.2 and 0.3 mol. wt. % composites are 1339.83 cm^{-1} for x = 0.2 and 1337.81 cm^{-1} for x = 0.3 mol. wt. %. The only noticeable peaks in xz polarization and E symmetry is at 498.82 cm^{-1} and the 1091.76 cm^{-1} shoulder appears to be weak in xx, zz and xz polarization making it likely that at least some of the peaks causing this feature would be maximized in the xy polarization and therefore of B symmetry in x = 0.1 mol. wt. %. E symmetry peaks are found in x = 0.2 and 0.3 are at 508.90 cm^{-1} and 496.80 cm^{-1}. The shoulder peaks appears in x = 0.2 and 0.3 are at 1029.24 and 1117.98 cm^{-1} respectively. The E peaks leaves some weak peaks at 686.38, 783.19 and 829.19 cm^{-1} in x = 0.1 which shifted in x = 0.2 and 0.3 are at 686.38, 752.94 and 851.39 cm^{-1} and 674.38, 775.94, 873.38 cm^{-1} respectively (Table 4).

Unassigned and a speculatively assignment for the 1091.76 cm^{-1} feature. CdI_2 contamination peaks also found in at 2854.45, 2854.45 and 2842.35 cm^{-1} for x = 0.1, 0.2 and 0.3 respectively. Peaks of B and E symmetry are allowed in the IR spectra and should be strong peaks. The occurrence of 498.82 cm^{-1} for [Cu_2CdI_4:0.xRbI] in the IR strengthens the E assignment for the peak at 442.45 cm^{-1}. For the x = 0.2 and 0.3, the peaks are at 454.52 and 442.48 cm^{-1} in [Cu_2CdI_4:0.xRbI] respectively (Table 4).

3.1.3. FTIR Comparison in Cu_2CdI_4

From Table 3, the vibrational modes can be assigned by considering Cu_2CdI_4 as consisting of the vibrational modes of AgI and $(CdI_4)^{2-}$ species. In fact, as shown in Fig. 2, almost all the bands due to AgI and $(CdI_4)^{2-}$ are seen in the pure Cu_2CdI_4 composites. The band at 1614.11 cm^{-1} can be assigned to the symmetric stretching "A" mode of $(CdI_4)^{2-}$ species and this band is the strongest band at room temperature [24].This assignment is in good agreement with the other $(CdI_4)^{2-}$ tetrahedral compounds [26]. On the doping of (0.1RbI) ions in the [Cu_2CdI_4:0.1RbI], all ten bands shifted to 442.45, 498.82, 686.38, 783.19, 829.19, 952.60, 1091.76, 1349.91, 1614.11 and 3572.43 cm^{-1}. The 1000 - 1500 cm^{-1} region consists of two bands at the positions 1091.76 cm^{-1} and 1349.91 cm^{-1} at room temperature and at low temperature, these bands are expected to split. It is known from the IR spectra of [0.1RbI]- ions conductors that this region consists of mostly of Ag-I [27] stretching modes. Hence, in all [Cu_2CdI_4:0.1RbI] composite samples, also the bands in this region can be assigned to symmetric stretching modes of Ag-I. Below 700 cm^{-1}, there are five sharp bands at 442.45, 498.82, 686.38, 783.19, 829.19 cm^{-1} in [Cu_2CdI_4:0.1RbI] [24], while species vibrations, the bands at 454.52, 508.90, 686.38, 752.94, 851.39 cm^{-1} and 442.48, 496.80 674.38, 775.94, 873.38 cm^{-1} in x = 0.2 and 0.3 (Rb^+)-ions conductors respectively, it is known from factor group analysis studies [20] that the bands in this region are due to deformation type metal-iodine vibrations. On comparison with $(CdI_4)^{2-}$ species vibrations, the bands at 442.45 and 686.38 cm^{-1} in [Cu_2CdI_4:0.1RbI] are at 454.52 cm^{-1} and 686.38 cm^{-1} in x = 0.2 and 442.48 cm^{-1} and 674.38 in x = 0.3 (Rb^+)-ions conductors respectively can be assigned to Cd-I deformation type bands. The band at 475.20 cm^{-1} in pure Cu_2CdI_4, and 498.82, 508.90 and 496.80 cm^{-1} in x = 0.1, 0.2 and 0.3 mol. wt. % (Rb^+)-doped ions conductors respectively, is attributed to the E symmetry of Rb^+ translational mode and is the

characteristic attempt frequency of Rb^+ ion arising from the diffusive behavior to oscillatory behavior. This assignment is well explained by Shriver [28] by referring to the negative pressure dependence and also using theoretical calculations. The value assigned to the attempt frequencies in Cu_2CdI_4 is similar to cation transition modes in other related (Rb^+)-doped fast ionic conductors [28, 24]. Another possibility is that motion of very large amplitude (diffusive like) is able to create configurationally disorder which allows all IR modes [29].

Inspection of Table 3 and Fig. 2, shows that IR spectra of all [Cu_2CdI_4:0.xRbI] and conductors exhibit the strongest feature at ca 1614.11, 1604.03 and 1614.11 cm^{-1} respectively, while the infrared activity below 900 cm^{-1} is weak. On the basis of the above discussion, these results strongly suggest that the existence of $(CdI_4)_2^{2-}$ /(Rb^+) tetrahedral in the x = 0.1, 0.2 and 0.3 mol. wt. % (Ag^+:Cu^+)-doped fast ionic conductors should be excluded at least in concentration detectable by infrared spectroscopy.

Therefore, it is found that the infrared activity of the x = 0.1, 0.2 and 0.3 mol. wt. % (Rb^+)-fast ionic conductors arises from $(CdI_4)^{2-}$ tetrahedral. Increasing the Rb^+ content induces a decreases to increase of the infrared activity in [Cu_2CdI_4:0.x RbI] [24].

3.2. Scanning electron microscopic (SEM) Studies

The scanning electron microscopic (SEM) studies were performed to get information about homogeneity, particle distribution and morphology of all the fast ionic composite systems [Cu_2CdI_4:xRbI] (where x = 0.1, 0.2 and 0.3 mol. wt. %) after the reaction was completed (sintered) at room temperature. Fig. 3. shows typical results at two different magnifications (at 3000x and 10,000x), which clearly indicates the highly agglomerated nature of particles. The average size of agglomerated particles is 1.5–1.99 μm in diameter. Here it may be noted that the agglomeration is more obvious at higher magnification (Fig. 3b). Further, there is a distinct possibility of existence of nanosize amorphous particles. The sintering temperature of all the samples cannot be high enough to synthesize the pure phase of monoclinic [Cu_2CdI_4:xRbI] sample as indicated by FTIR. The sem images shown in Fig. 3 suggest that the particles of all the samples sintered at particular temperature are covered with a slice of RbI which are attributed to the residual RbI particles left over from the solid state reaction method [30]. The residual RbI particles can favor stabilization of Cd^{2+} and facilitate the diffusion of Cu^+. This is to say, it is the result as a consequence of Cu_2CdI_4 decompositions during preheating and sintering process and produces a composite powder [Cu_2CdI_4:xRbI] with superior conductivity [31].

However particular temperature (100ºC) preparation causes the absupt growth of particles with a smooth surface particle of ≈ 1.5–1.99. It has been reported that the morphology and surface area of obtained particles have a notable effect on the electrochemical performance of [Cu_2CdI_4:xRbI] and optimizing particle size or introducing conducting additives can improve the performance [32]. As nanometer size RbI particles can be dispersed uniformely between [Cu_2CdI_4] particles. It has played a beneficial role in obtaining samples with small and uniform particles size and enhancing overall conductivity. Furthermore, solid state reaction method can prevent particles from agglomeration.

3.3. EDAX

Chemical analysis of a few processed samples was carried out by EDAX to check if there is any deviation from the initial composition. Fig. 4 shows a typical EDAX result for [Cu_2CdI_4:0.xRbI] (were x = 0.1, 0.2 and 0.3 mol. wt. %) sample. In a [Cu_2CdI_4:0.xRbI] (were x = 0.1, 0.2 and 0.3 mol. wt. %) samples shows a typical EDAX result, the wt. % of the four elements (Cu = 20.34%, Cd = 13.28%, Rb = 1.65%, I = 64.73%)) in a [Cu_2CdI_4:0.1RbI], whereas the wt. % of the four elements (Cu = 13.75%, Cd = 16.26%, Rb = 3.51%, I = 66.48%) and (Cu= 16.58%, Cd = 10.60%, Rb = 8.61%, I = 64.21%) in a x = 0.2 and 0.3 mol. wt. % respectively, is nearly same as in the unprocessed (Cu = 20%, Cd = 13%, Rb = 7%, I = 65%) material. It is thus concluded that the formation of all the fast ion conductors by solid state reaction does not alter the composition of the samples [33, 34].

4. Conclusion

A novel composite superionic systems [Cu_2CdI_4:0.xRbI] (were x = 0.1, 0.2 and 0.3 mol. wt. %), were investigated. An alternative ternary system [Cu_2CdI_4] was used as host. In the host [Cu_2CdI_4] structure, doping with Rb^+ in the host induces a decrease in the mobile charge carriers, Rb^+ ions that is proportionate with the increased 0.x mol. wt. % (x = 0.1, 0.2 and 0.3 mol. wt. %) in the host mixed system.

FAR-IR, FTIR, SEM and EDX studies confirmed the formation of a superionic phase in the composite system.

5. Acknowledgements

The authors are gratefully acknowledged to UGC New Delhi for financial assistance as UGC-PDF Women Scientist Scheme. The authors also gratefully acknowledge the Chairman of the Department of Chemistry for providing the research facilities.

References

[1]. Goodenough J B. Ceramic solid electrolytes, Solid state ionics. 94; 1997: 17-25.
[2]. Geller S (ed). Solid Electrolytes (Berlin Springer) 1977.
[3]. Hull S. Superionics: crystal structures and conduction processes. Rep. Prog. Phys. 67; 2004: 1233-1314.
[4]. Agrawal R C, Gupta R K. Transport property and battery discharge characteristic studies on $1-x$ $(0.75AgI{:}0.25AgCl){:}xAl_2O_3$ composite electrolyte system. Journal of Materials Science. 30; 1995: 3612-3618.
[5]. Beeken R B, Faludi J. C., Schreier W M, Tritz J M. Ionic conductivity in Cu-substituted Ag2CdI4. Solid State Ionics. 154-155; 2002: 719-722.
[6]. Matsui T and Wagner J B. High Conductivity Cuprous Halide-Metal Halide Systems. **Jr. J. Electrochem. Soc**. 124; 1977: 937-940.
[7]. Khalid Siraj, Rafiuddin, Effect of cation substitution on the conductivity of Cu_2CdI_4, European Journal of Scientific Research, Vol 50, No 2 (2011), pp 187-190.
[8]. Kennedy J H, Schaupp C, Yang Y and Zhang Z. Composition and Properties of Thallium Mercury Iodide. J. Solid State Chem. 88; 1990: 555-563.
[9]. Noorussaba and Afaq Ahmad, Synthesis, Infrared spectroscopic and Thermal studies of $[0.7(Cu_2CdI_4){:}0.3(AgI_x{:}CuI_{(1-x)})]$ of fast-ion conductor (x = 0.2, 0.4, 0.6 and 0.8 mol. wt. %), Asian J. Research Chem. 8(2): February 2015.
[10]. Noorussaba and A. Ahmad, Anal. Bioanal. Electrochem., 2011, 3, 261-278.
[11]. R. C. Agrawal, R. Kumar, A. Chandra, Sol. Stat. Lonics, 1996, 84, 51.
[12]. V.P. Glushko, L.V. Gurvich, G.A. Bergman, I.V. Veits, V.A. Medvedev, G.A. Khachkuruzov and V.S. Yungman, Termodinamicheskie Svoista Individual nykh Veshchestv, Vol I V, Nauka, Moskow, 1982.
[13]. B.T. Gowda and S.W. Benson, J. Chem. Soc., Faraday Trans. 2, 79, (1983) 663.
[14]. P. A. Akashin and V.P. Spiridonov, Kristallographia, 2 (1957) 472.
[15]. M.W. Listen and L.E. Sutton, Trans. Faraday Soc., 37 (1941) 406.
[16]. O. Hassel and L.C. Stromme, Z. Phys. Chem., 38 (1938) 466.
[17]. R. Viswanathan and K. Hilpert, Ber. Bunsenges. Phys. Chem., 83 (1984) 125.
[18]. H. W. Zandbergen, The crystal structure of α-thallium hexaiodochromate, α-Tl_4CrI_6, Acta Cryst. B., 35 (1979), pp. 2852-2855.
[19]. A.V.Franiv, O.S.Kushnir, I.S.Girnyk,V.A.Franiv, I.Kityk, M. Piasecki and K.J.Plucinski, Growth and optical anisotropy of Tl_4CdI_6 single crystals, Ukr. J. Opt, 14, 2013, pp. 6-13.
[20]. D. S. Kalyagin, Yu. E.Ermolenko and Yu. G.Vlasov, Diffusion of Tl-204 isotope and ionic conductivity in Tl_4 HgI_6 membrane material for chemical sensors, Rus. J. appld Chem., 81 (2008), pp. 2172-2174.
[21]. M. Hassan, M. S. Nawaz and Rafiuddin, Ionic conduction and effect of immobile cation substitution in binary system (AgI) 4/5–(PbI2) 1/5, Radiation effects and defects in Solids,163 (2008), 11, pp. 885-891.
[22]. K. Wakamura, Characteristic properties of dielectric and electronic structures in super ionic conductors, Solid state ionics, 149 (2002), pp. 73–80
[23]. R. Sudharsanan, T.K.K. Srinivasan and Radhakrishna, Raman and far IR studies on Ag_2CdI_4 and Cu_2CdI_4 superionic compounds, Solid. state. ionics. 13 (1984), pp. 277-283 North-Holland, Amsterdam
[24]. E. A. Secco, A. Sharma, Structure stabilization: locking-in fast cation conductivity phase in TlI, J Phys Chem Sol, 2 (1995), pp. 251–254.
[25]. N.F. Uvarov, P. Vanek, Yu.I. Yuzyuk, V. Zelezný, V. Studnicka, B.B. Bokhonov, V.E. Dulepov and J. Petzelt, Properties of rubidium nitrate in ion-conducting $RbNO_3$-Al_2O_3 nanocomposites, Sol. Stat. Ionics 90 (1996), pp. 201-207.
[26]. J. B. Goodenough, Ceramic solid electrolytes, Solid State Ionics, 1997, 94, 17-25
[27]. S. Beg, N.A.S. Al-Areqi and S. Haneef, Study of phase transition and ionic conductivity changes of Cd-substituted $Bi_4V_2O_{11-\delta}$, Sol. Stat. Ionics 179 (2008), pp. 2260–2264.
[28]. A. Viswanathan, S. Austin Suthanthiraraj, Impedance and modulus spectroscopic studies on the fast ion conducting system CuI-Ag_2MoO_4,, Solid State Ionics, 62, 1–2 (1993), pp. 79-83

[29]. E. Kartini, T. Sakuma, K. Basar, M. Ihsan, Mixed cation effect on silver–lithium solid electrolyte $(AgI)_{0.5}(LiPO_3)_{0.5}$, Sol. Stat. Ionics 179 (2008), pp. 706–711.
[30]. [30] X. J. Zhu, Y. X. Liu, L. M. Geng, L. B. Chen, Synthesis and performance of lithium vanadium phosphate as cathode materials for lithium ion batteries by a sol-gel method, J. of power sources 184 (2008) 578-582.
Y. Hu. Y.H. Liu, ----------Mater. Chem. Phys. 90 (2005) 255.
[31]. P. Fu, Y. Zhao, Y. Dong, X. An, G. Shen, J. of power sources 162 (2006) 651.
[32]. X. Zhu, Y. Liu, L. Geng, L. Chen, H. Liu, M. Cao, Solid state ionics 179 (2008) 1679.
[33]. Xianjun Zhu, Yunxia Liu, Liangmei Geng, Longbin Chen, Hanxing Liu, Mingle Cao, Synthesis and characteristic of Li3V2(Po4) as cathode materials for lithium-ion batteries, solid state ionics, 179 (2008) 1679-1682.
[34]. Khalid Siraj, Rafiuddin, Soft Nanosci. Lett., 2, 2012, 13-16.

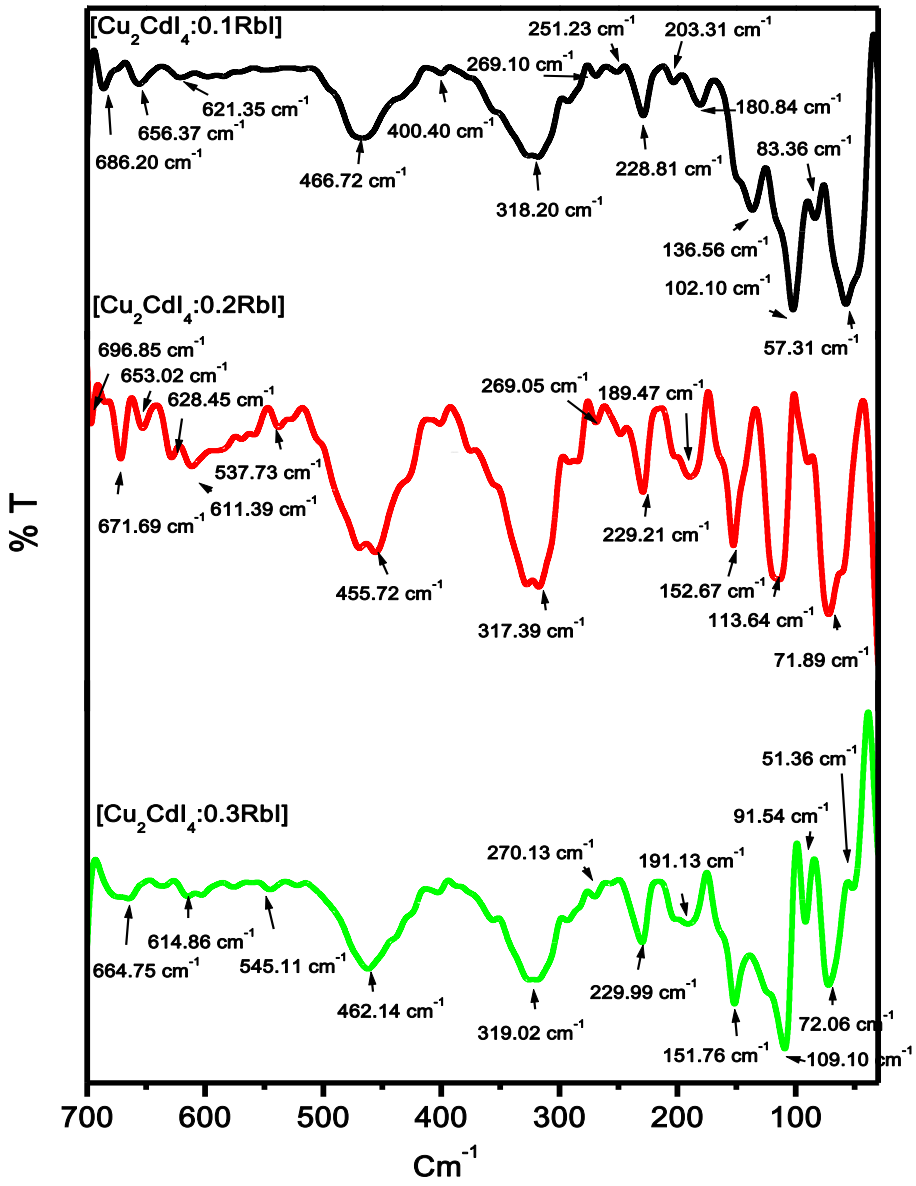

Fig. 1. FAR-IR spectrum for $[Cu_2CdI_4:0.xRbI]$ fast ionic conductors

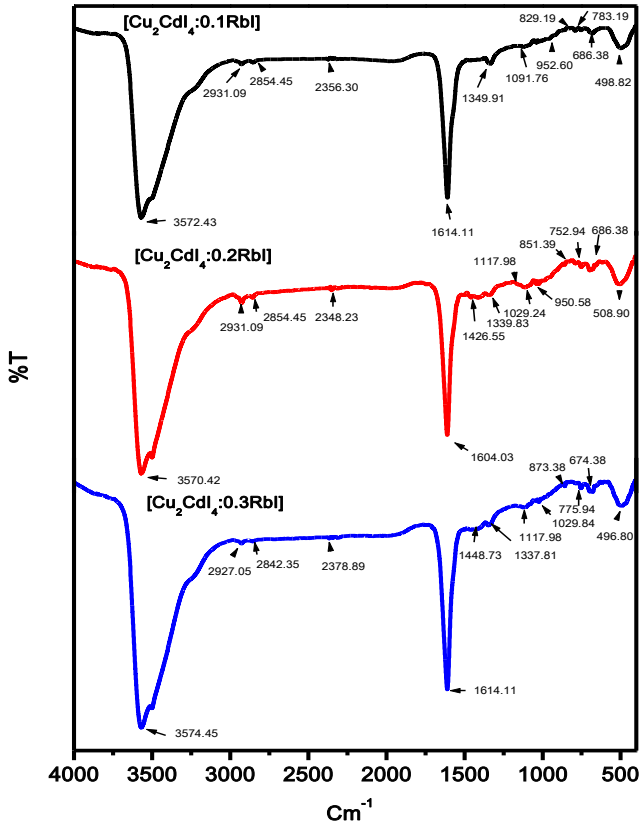

Fig. 2. FTIR spectrum for [Cu_2CdI_4:0.xRbI] fast ionic conductors.

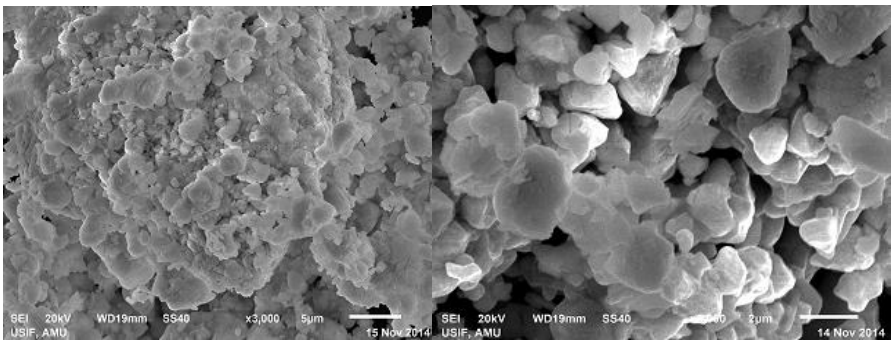

(a) **(b)**

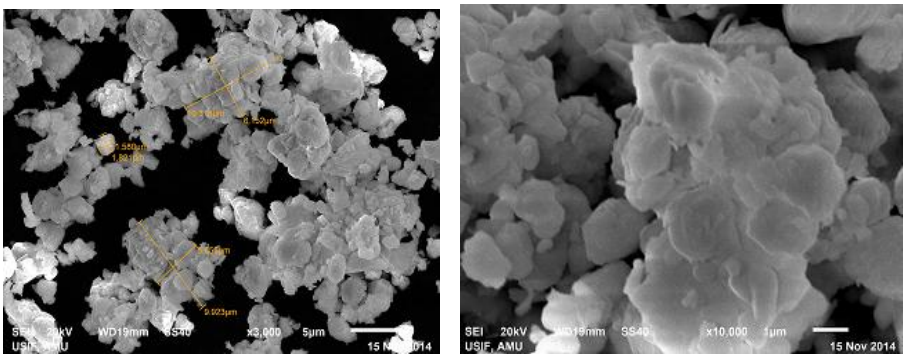

(c) **(d)**

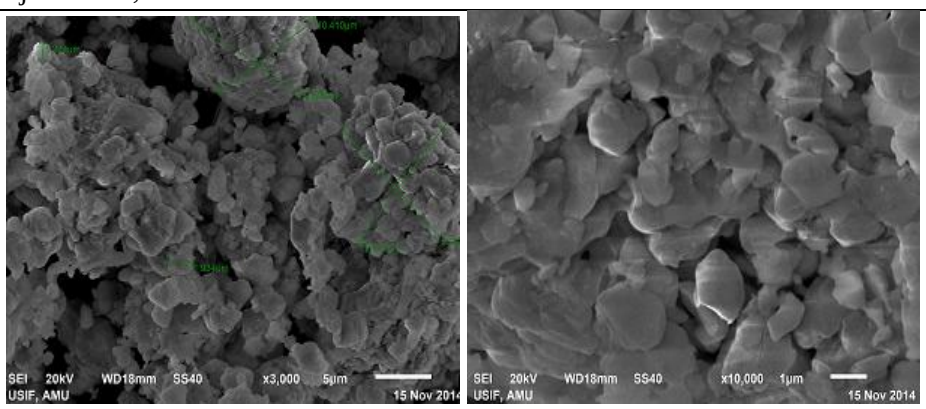

(e) **(f)**

Fig. 3. SEM photographs of (a) [Cu_2CdI_4:0.1RbI] at 3000x and (b) at 10,000 x, (c) [Cu_2CdI_4:0.2RbI] at 3000x and (d) at 10,000 x, (e) [Cu_2CdI_4:0.3RbI] at 3000x and (f) at 10,000 x respectively. The particles are seen in a highly agglomerated state. The typical agglomerated particle size is in the range 1.5–1.99 μm

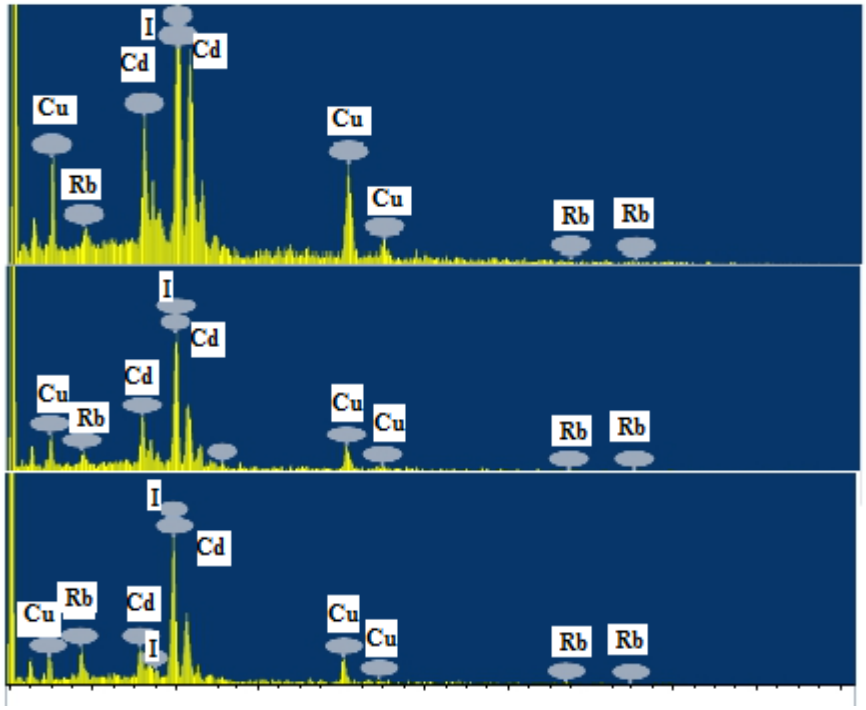

Fig.4. EDAX results for [Cu_2CdI_4:xRbI] sample. Showing the presence of elements (Cu, Cd, Rb, I). The inset shows weight/atomic ratios of the four elements present in the sample are same as that in the unprocessed sample.

International Journal of Recent Engineering Research and Development (IJRERD)
Volume No. 02 – Issue No. 01, ISSN: 2455-8761
www.ijrerd.com, PP. 31-41

Table 1. FAR-IR bands in [Cu_2CdI_4:0.xRbI] and assignments

Compound	[Cu_2CdI_4:0.1RbI]	[Cu_2CdI_4:0.2RbI]	[Cu_2CdI_4:0.3RbI]	Assignments	nature
CuI	102..10 83.36 57.31	113.64 71.89 ------	109.10 91.54 72.06 51.36	ω_e B_{2u} and B_{3v} B_{1u}	CuI stretch of the nonomer stretching motion of $(CuI)_2$ dimeric molecule bending motion of the $(CuI)_2$ molecule
CdI_2	228.81 136.56	229.21 152.67	229.99 151.76	υ_3 υ_2	symmetric Cd-I stretch of the dimer I- Cd-I blend
Cu_2CdI_4	318.20, 466.72 621.35	317.39, 455.72 628.45	319.02, 469.14 614.86	- - -	Dissociation of the [Cu_2CdI_4]molecule Cu-I stretch $(CdI_2)_2$ stretch
RbI Cu_2CdI_4-RbI	203.31, 251.23 269.10 656.37 686.20	189.47 269.05 — 537.73 611.39 653.02 671.69	191.13 270.13 — 545.11 664.75	— — — — —	RbI-I stretch of the molecule RbI-I stretch of the molecule formation of the [Cu_2CdI_4:0.xRbI] band formation of the [Cu_2CdI_4:0.xRbI] band formation of the [Cu_2CdI_4:0. xRbI] band

Table 2. [Cu_2CdI_4:0.xRbI] fast ion conductors, where (x = 0.1, 0.2 and 0.3 mol. wt. %) room temperature peaks and assignments.

[Cu_2CdI_4:0.xRbI]		[Cu_2CdI_4:0.xRbI]		[Cu_2CdI_4:0.xRbI]	
Peaks (cm^{-1})	Assignments	Peaks (cm^{-1})	Assignments	Peaks (cm^{-1})	Assignments
2931.09	A	2931.09	A	2941.17	A
1614.11	A	1604.03	A	1614.11	A
1091.76	?	1029.24	?	1029.84	?
1349.91	B	1339.83	B	1337.81	B
498.82	B	508.91	B	496.80	B

Table 3. [Cu_2CdI_4:0.xRbI] fast ion conductors, where (x = 0.1, 0.2 and 0.3 mol. wt. %) room temperature peaks and assignment.

FTIR transmission peaks (cm^{-1})				
[Cu_2CdI_4:0.1RbI]	**[Cu_2CdI_4:0.2RbI]**	**[Cu_2CdI_4:0.3RbI]**	**Symmetry**	**Assignment**
1614.11	1604.03	1614.11	A	CdI_4^{2-} deformation, M-I stretching
1091.76	1029.24	1029.84	B	deformation
1349.91	1339.83	1337.81	E	Cu-I , Cu-I symmetric stretch
498.82	508.91	496.80	E	Cu^+ , Rb^+ attempt frequency

Table 4. [Cu_2CdI_4:0.xRbI] fast ion conductors, where (x = 0.1, 0.2 and 0.3 mol. wt. %), room temperature peaks and assignment.

FTIR -transmission (cm^{-1})				Assignment
Pure [Cu_2CdI_4]	**[Cu_2CdI_4:0.1RbI]**	**[Cu_2CdI_4: 0.2RbI]**	**[Cu_2CdI_4:0.3RbI]**	
475.20 439.02 420.16 521.90 490.00 1624.13	498.82 ----- 686.38 533.65 2356.30 783.19 1614.11	508.91 429.52 686.38 510.09 2348.23 752.94 1604.03	496.80 437.78 674.38 567.90 2378.89 775.94 1614.11	Cu -I deformation Cd-I deformation Rb-I symmetric stretch $(CdI_4)^{2-}$- I symmetric stretch